INTERNATIONAL JOURNAL FOR NUMERICAL METHODS IN FLUIDS
Int. J. Numer. Meth. Fluids 2010; **63**:1147–1166
Published online 23 July 2009 in Wiley InterScience (www.interscience.wiley.com). DOI: 10.1002/fld.2124

An evolutionary optimization of diffuser shapes based on CFD simulations

S. Ghosh, D. K. Pratihar*,†, B. Maiti and P. K. Das

Indian Institute of Technology, Kharagpur 721302, India

SUMMARY

An efficient and robust algorithm is presented for the optimum design of plane symmetric diffusers handling incompressible turbulent flow. The indigenously developed algorithm uses the CFD software: Fluent for the hydrodynamic analysis and employs a genetic algorithm (GA) for optimization. For a prescribed inlet velocity and outlet pressure, pressure recovery coefficient C_p^* (the objective function) is estimated computationally for various design options. The CFD software and the GA have been combined in a monolithic platform for a fully automated operation using some special control commands. Based on the developed algorithm, an extensive exercise has been made to optimize the diffuser shape. Different methodologies have been adopted to create a large number of design options. Interestingly, not much difference has been noted in the optimum C_p^* values obtained through different approaches. However, in all the approaches, a better design has been obtained through a proper selection of the number of design variables. Finally, the effect of diffuser length on the optimum shape has also been studied. Copyright © 2009 John Wiley & Sons, Ltd.

Received 3 March 2009; Revised 10 June 2009; Accepted 10 June 2009

KEY WORDS: incompressible flow; optimization; genetic algorithm; 2D planar diffuser; 2D planar duct

1. INTRODUCTION

Optimization has become an inseparable step of the design process in many of the engineering systems. From the engineering point of view, the main motive for the optimum design has been a reduction in the initial cost, operating cost or both under a set of constraints, which are dictated by the diverse parameters such as process requirements, available infrastructure, safety, environmental concern, etc. Based on the above goal, a set of design variables is optimized. For a thermo-fluid system, such relevant output variables could be shear stress in biomems, efficiency of a pump, rate of heat transfer in a cooling system, drag of a car body or pressure drop in a pipe network.

*Correspondence to: D. K. Pratihar, Indian Institute of Technology, Kharagpur 721302, India.
†E-mail: dkpra@mech.iitkgp.ernet.in

Such optimization exercise not only aims to find out the suitable process parameters but also often seeks the optimum shape of the physical system.

Shape optimization is a classical problem. From time immemorial, it was known that a curve of a given length encompasses the largest area if it becomes a circle. One can also refer to the Brachistochrone problem, which was posed to the then scientific community by Johann Bernoulli in 1696 [1]. In this problem, one needs to find out the shape of the curved path between two points in a vertical plane such that a point mass takes the minimum time to slide along it. Even a genius like Sir Isac Newton was attracted to the mathematical rigor of the problem and the result was the beginning of calculus of variation! [1, 2]. Over the years, various shape optimization problems have been taken up by the scientific and engineering community. As the present work is concerned with the optimum design of a fluid flow system, a brief overview of some of the shape optimization exercises in thermo-fluids engineering is given below.

2. LITERATURE SURVEY

The process of optimization for thermo-fluidic systems most often contains two steps. The objective function is computed from the hydrodynamic and heat transfer simulations through various analytical or numerical methods. An optimization algorithm is used next to determine the design variables that optimize the objective function. Again, diverse techniques of optimization ranging from classical gradient-based methods and search algorithms to evolutionary programs are in use. Fabbri employed a genetic algorithm (GA) for the optimization of both corrugated wall channel [3] as well as internally finned tubes [4, 5]. Arrangement and determination of optimal shapes for staggered pin fins in the channel of a plate heat exchanger were attempted by Lee *et al.* [6]. A numerical and experimental geometric optimization for general staggered configurations had been studied in [7] to maximize the total heat transfer rate among a bundle of finned or non-finned tubes in a given volume. By using various multi-objective optimization methods, optimal results for a micro-heat-exchanger had been obtained in [8].

A large volume of work had been carried out on shape optimization of fluid flow systems relevant to aerodynamics applications [9, 10]. Falco [11] carried out the optimization of aerofoil shapes using evolutionary algorithms. Multi-objective design optimization in aerodynamics and electromagnetics was conducted by Makinen *et al.* [12]. Several non-linear optimization problems related to general fluid flow had been solved using gradient-based optimization tools by various investigators [13–17]. A shape optimization of cutoff in a multi-blade fan/scroll system was done by Han and Maeng [18] using two-dimensional CFD. A flow solver and a mathematical optimization tool (implementation of a trust region-based derivative-free method) were combined and used as an integrated procedure by Lehnhauser and Schafer [19] for the shape optimization of a fluid flow domain.

Diffusers are the integral parts of many flow systems. An improperly designed diffuser may lead to flow separation and excessive consumption of pumping power. It may also produce a flow mal-distribution in the downstream, which is not acceptable in many applications. Moreover, a constraint of restricted length is often imposed on the design. As a result, designing the optimum shape of a diffuser had been the subject of investigation for many researchers during the last decade. Optimum design of a straight-walled diffuser was obtained by Kline *et al.* [20]. Four common optimization problems were analyzed and optimal solutions were located in relation to the overall flow regimes in terms of geometrical parameters for the straight-walled unit. The

DOI: 10.1002/fld

performance of a straight two-dimensional diffuser had been studied and analyzed by Reneau *et al.* [21]. The effect of wall shape on flow regimes and performance had been studied in a straight two-dimensional diffuser by Carlson *et al.* [22]. The profile of a plane diffuser with given upstream width and length had been optimized to obtain the maximum static pressure rise by Cabuk and Modi [23]. The steady-state Navier–Stokes equation was used to model the flow through the diffuser considering two dimensional, incompressible and laminar flow. A set of adjoint equations had been solved to get the direction and relative magnitude of change in the diffuser profile that leads to a higher pressure rise. Repeated modification of the diffuser geometry with each solution to the direct and adjoint set of partial differential equations leads to a diffuser with the maximum static pressure rise. Geometries for three-dimensional viscous flow had been optimized by Svenningsen *et al.* [24], applying quasi-analytical sensitivity analysis. The optimization tool had been applied on a two-dimensional laminar diffuser in order to maximize the pressure recovery by contouring the divergent wall section and the performance of the diffuser was found to improve by about 5% compared with that of straight-walled geometry. A response surface technique had been used to optimize the shape of a two-dimensional diffuser subjected to incompressible turbulent flow by Madsen *et al.* [25]. The shape of diffuser wall was described using polynomial and B-splines with two and five design variables, respectively. They also applied monotonicity condition, which drastically reduced the design space. Growth-strain method was used for shape optimization in a flow system by Maeng and Han [26]. They have optimized the shape by assuming a distributed parameter-like dissipation energy to be uniform in a flow system. A diffuser had been optimized using the support vector mechanics (SVM) by Fan *et al.* [27]. The SVM was used to construct a response surface. In that study, the optimization was performed on an easily computable surrogate space. Shape optimization was carried out by Goel *et al.* [28] to improve hydrodynamic performance of diffuser vanes of a pump stage. Bezier curves and circular arcs had been used to define the shape of the vanes. To identify the regions of the vane that have a strong influence on its performance, surrogate model-based tools were used. In the absence of manufacturing and stress constraints, optimization of the vane shape led to a nearly 8% reduction in the total pressure losses compared with the baseline design by reducing the base separation.

In the present work, the shape optimization of a two-dimensional symmetric diffuser has been considered. Commercial softwares, namely Fluent [29] and Gambit [30] have been used to analyze the hydrodynamics. However, one needs to be cautious in selecting the optimization technique for the present nature of the problem. Techniques based on gradient search and direct search are powerful methodologies of optimization [31]. In the direct search, the search starts with randomly generated initial solutions and the final optimal solution might depend on the chosen initial solutions. The gradient-based method cannot be applied for a problem involving discontinuous objective function space. Further, the chance of the gradient-based method for getting stuck at the local extremum cannot be ruled out.

The optimization algorithms based on evolutionary principle can eliminate some of the difficulties listed above, as they work on a methodology completely different from those of classical techniques. For instance, GA, which loosely mimics genetic evolution following the principle of natural selection [32, 33], offers a number of unique flexibilities. This robust and generic search technique can handle continuous as well as discrete variables while assuring a global optimization. It also provides a several near-optimal solutions, which offer the designer a large number of options. The use of a GA coupled with a CFD-based modeling possesses enough promise to solve shape optimization of systems involving fluid flow.

DOI: 10.1002/fld

Based on the above observation, a GA has been utilized for the optimization. Through the use of unique system commands, Gambit, Fluent and GA have been integrated into a single algorithm. The developed program facilitates the exchanges of data among the commercial softwares and the optimization code in a fully automated manner. A number of alternate methodologies have been used to generate the optimum profiles. A critical comparison of all the methods has been made. Finally, a comprehensive investigation has also been done to explore the effect of different design parameters on the optimum shape.

The rest of the text has been organized as follows: Section 3 deals with the statement of the problem. The proposed methodology is explained in Section 4. Results are stated and discussed in Section 5. Some concluding remarks are made in Section 6.

3. PROBLEM STATEMENTS

A diffuser is generally used either to recover static pressure or to minimize total pressure loss in a pipe or in a duct. The aim of the present problem is to determine the optimum shape of a symmetric two-dimensional planar diffuser (schematically shown in Figure 1) to achieve the above goal.

An incompressible fluid enters the domain with a uniform velocity. It is required to diverge the flow passage to the double of its width. The flow through the diffuser is assumed to be fully turbulent with Reynolds number of 10^5, based on the inlet half-width of the diffuser d. The model considers symmetry condition along the channel axis. Solving the fluid flow problem, one can find out the velocity and pressure fields from the inlet to the outlet. The performance of the diffuser can be expressed in terms of non-dimensional pressure recovery factor C_p^*, as given in Equation (1).

$$C_p^* = \frac{\Delta p}{\frac{1}{2}\rho v_{\text{inl}}^2} \tag{1}$$

where Δp represents the gain in static pressure, ρ indicates the density of the fluid and v_{inl} denotes the inlet velocity of the fluid flow. Therefore, the problem boils down in finding out the appropriate shape of the curve *abc* (refer to Figure 1) to yield the maximum value of C_p^*. Two non-dimensional parameters, namely ratio of inlet to outlet area (A_r) and the ratio of the length of the diffuser to the inlet throat half-width (l/d), may be used as the key parameters for the design of the diffuser.

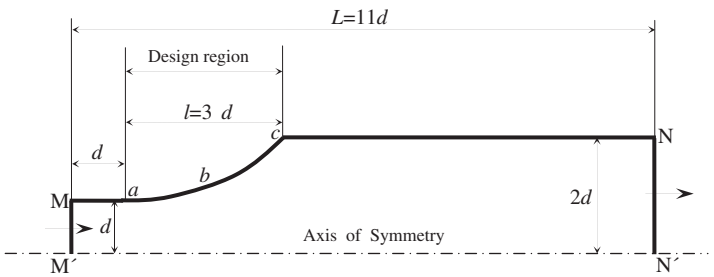

Figure 1. One half of a planar symmetric diffuser.

DOI: 10.1002/fld

In the present problem, the values of A_r and l/d are kept fixed at 2.0 and 3.0, respectively. The total length of the duct is $11d$ (where d indicates the half-width of inlet throat) and the horizontal length of the inlet section is assumed to be equal to $1d$. It is important to mention that such a long length after the diffuser has been considered to *ensure* a proper development of the flow.

4. METHODOLOGY

The adopted methodology of optimization has three main components. First, one needs to solve the hydrodynamics of the diffuser for determining the C_p^*, which is considered as the objective function during optimization. One also requires to design the optimization algorithm (GA in the present case) such that the objective function is optimized for the given set of constraints. Last but not the least; one needs to devise a computational algorithm that will combine the CFD software with the GA in a monolithic platform for a fully automated operation.

4.1. Hydrodynamic calculation

The best design of diffuser should have a maximum C_p^*. To find out C_p^*, one needs to solve the mass and momentum conservation equations along with appropriate boundary conditions for a given geometry of the diffuser. The commercial CFD software, Fluent 6.3.26 [29], has been used for this purpose. It discretizes the conservation equations by a finite volume technique and solves them. The mesh for the discretization has been created by a software called Gambit [30]. The standard k–ε model [34] has been used for turbulence modeling. Further, in order to capture the wall effect accurately the standard wall function proposed by Launder and Spalding [35] has been used. The velocity inlet (MM' in Figure 1) boundary condition is considered, while a pressure outlet condition relaxing to atmospheric pressure is imposed at the exit (NN$'$ in Figure 1). The condition of symmetry is applied at the bottom boundary (M$'$N$'$ in Figure 1) and wall condition is used on the top boundary (MabcN in Figure 1). The number of grids has been decided after conducting a grid-independence test. The normalized residuals are computed at each iteration by the Fluent. Once all of these residuals fall below a prescribed value, it is assumed that convergence has been reached. In this study, fixed values of 3×10^{-6} for the continuity residual and 1×10^{-6} for the x-velocity, y-velocity, k and ε residuals are used.

4.2. GA implementation

A GA has been used here for the optimization of the diffuser. The principle of GA has been explained in details in [31–33]. Only a brief outline is presented here. The GA starts with a population of possible solutions (that is, different options of diffuser geometry in the present case), which are generated at random. Let us assume that a GA-string carries information of four control points used to decide the wall shape of the diffuser. As the x and y coordinates of four control points are independently evaluated from the GA-string, there are eight variables (four x positions and four y positions) coded within the chromosome. The field size for each variable is chosen as 20. As there are eight variables, the total length of the chromosome will be equal to 160.

DOI: 10.1002/fld

A particular GA-string will look as follows:

$$\underbrace{10001101110001001110}_{x_1}\underbrace{11001010011101001010}_{x_2}\underbrace{11110011100100001000}_{x_3}$$

$$\underbrace{11100000110110101101}_{x_4}\underbrace{00011111001001111100}_{y_1}\underbrace{01001101110010011010}_{y_2}$$

$$\underbrace{10001100000000010011}_{y_3}\underbrace{11011001011010001001}_{y_4}$$

The first 20 bits, that is, (10001101110001001110) yields the decoded value (DV) as $1\times2^{19}+0\times2^{18}+0\times2^{17}+0\times2^{16}+1\times2^{15}+1\times2^{14}+0\times2^{13}+1\times2^{12}+1\times2^{11}+1\times2^{10}+0\times2^{9}+0\times2^{8}+0\times2^{7}+1\times2^{6}+0\times2^{5}+0\times2^{4}+1\times2^{3}+1\times2^{2}+1\times2^{1}+1\times2^{0}=580\,686$. The real value of x_1 can be determined following the linear mapping rules as given below:

$$x_1 = x_{1,\min} + \frac{x_{1,\max} - x_{1,\min}}{2^{\text{fieldsize}} - 1} \times \text{DV}$$

The real values of other variables can also be calculated following the similar procedure. After determining the real values of the design variables, the fitness values of all members of the population are calculated. In the present context, the fitness value is nothing but the pressure recovery coefficient of the diffuser for a particular design. The better solutions from the present population pool are selected for the next operations by the reproduction operator. In the present exercise, tournament selection has been used as the reproduction operator. It is important to mention that two players have been selected at random for the tournament. To exchange properties between two parents, crossover operator (namely uniform crossover) is used. Uniform crossover has been utilized in the present study, as it is generally found to be perform better than both simple point as well as two-point crossovers [31]. Mutation operator is then utilized to introduce some diversity in the solution space and to avoid convergence in the local optima. Once the new population is obtained through crossover, it is subjected to mutation to bring some local changes around the current solutions. The above basic steps are repeated for a large number of generations (specified *a priori*), so that globally optimized solutions are obtained.

The boundary and inlet conditions for this problem are kept the same for different simulations, and only the computational geometries have been varied. Various options for the geometry of the diffuser wall (curve *abc* of Figure 1) are generated by some design variables. These design variables are control points defined by the horizontal and vertical positions on the curve *abc* (in Figure 1). Selection of these design variables or control points is the most crucial task for the present study. Too many control variables may not guarantee the optimum solution but may complicate the optimization procedure and increase the computational time. Again, by using too few variables, a limited range of shape alternatives is obtained and the solution becomes biased. Therefore, a wide range of shapes defined by a relatively small number of parameters is appropriate for optimization. These design variables or control points represented by the GA-string are the sole input parameters from the GA to the CFD software.

To construct a curved wall like *abc* (refer to Figure 1), the mesh generating software: Gambit uses non-uniform rational basic spline (NURBS). Though an edge with a varying curvature can be defined by various different curves such as spline, Bezier; NURBS offers a number of flexibilities. As the NURBS uses a parametric functional relationship for the given control points, it does

DOI: 10.1002/fld

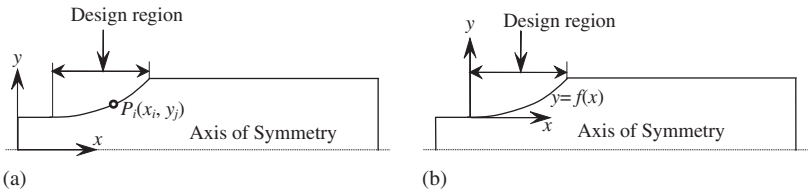

Figure 2. Coordinate systems for the control points: (a) directly chosen from GA and (b) generated using polynomial equation.

not face any difficulty in treating slopes of extreme values. Any geometrical complexity can be adequately captured, as the curve is represented by a number of low degree polynomials using a unique definition for the entire length. An NURBS curve of degree n is a piecewise rational polynomial function, wherein the numerator and denominator are non-periodic B-splines of degree n. Gambit provides with a computational implementation of the NURBS to generate the curves, when several points (referred to as control points) are specified. It is important to mention that for each subsequent GA fitness evaluation, the Fluent has been started with an initialized solution (that is, zero). Two different methodologies have been adopted in the present GA program to satisfy this requirement.

4.2.1. Direct selection of design variables. Here, the design variables or control points $P_i\ (x_i, y_i)$ derived from the GA-string may be directly used to construct the curve representing the wall shape. The x and y coordinates of control points are independently evaluated from the GA-string and transported to the Gambit for the construction of the NURBS curve. The positions of the control points are chosen with respect to a coordinate system, as shown in Figure 2(a). Attempts are made to determine optimal shape of the wall by varying the number of control points starting from one to six.

The coordinates of each control point are constrained by the upper and lower bounds. These upper and lower bounds vary with the number of control points or design variables used to construct the wall shape. The general form of the constraints for x coordinate is given below for all the six cases

$$\left[d+(m-1)\left(\frac{3d}{n}\right)\right]\leqslant x_m\leqslant\left[d+m\left(\frac{3d}{n}\right)\right] \tag{2}$$

where n and m are integers and

$$1\leqslant n\leqslant 6 \tag{3}$$

$$1\leqslant m\leqslant n \tag{4}$$

x_m denotes the x coordinate of the mth control point, where a total of n control points have been taken. The upper and lower bounds of y coordinates for all n control points have been kept the same, as expressed below

$$0.09d\leqslant y_m\leqslant 2.1d \tag{5}$$

Considering the fact that the y coordinates of the extreme ends of the diffuser (a and c in Figure 1) are $1.0d$ and $2.0d$, respectively, one may have taken $1.0d\leqslant y_m\leqslant 2.0d$. Instead, Equation (5) has been chosen to provide with a greater flexibility in design and give a larger search space for y_m.

DOI: 10.1002/fld

4.2.2. Selection of design variables using polynomial equation. In the next approach, the contour in the curved section of the diffuser wall has been described by a fourth-order polynomial function, as expressed below

$$y(x)=a_0+a_1x+a_2x^2+a_3x^3+a_4x^4 \tag{6}$$

where $y(x)$ denotes the vertical position of the curved wall corresponding to the axial position x (refer to Figure 2(b)). The curve starts at $x=0$ and ends at $x=3d$. Thus, the curve connects the points $(0,0)$ and $(3d, 1d)$. To make the selection of the control variables unbiased, the polynomial is parameterized in three different ways. At a and c (mentioned as inlet and outlet of the diffuser hereafter, as shown in Figure 1), there may or may not be the continuity of slope (denoted as C^1 continuity).

C^1 continuity at the inlet: Equation (6) contains five unknowns. For C^1 continuity at the inlet, the following conditions are to be satisfied: (i) at $x=0$, $y=0$; (ii) at $x=0$, $\mathrm{d}y/\mathrm{d}x=0$; (iii) at $x=3.0d$, $y=1.0d$. Two additional conditions are needed. One may consider two points on the curve wall equally spaced along the axial length and may introduce two design variables or control points as (iv) at $x=1.0d$, $y=y_1$ and (v) at $x=2.0d$, $y=y_2$. Thus, Equation (6) takes the form as given below

$$y(x)=a_2x^2+a_3x^3+a_4x^4 \tag{7}$$

Using the conditions (iii), (iv) and (v), the coefficients a_2, a_3 and a_4 can be expressed in terms of the design variables y_1 and y_2 as given below

$$a_2=\left(\frac{3.00}{d^2}\right)y_1-\left(\frac{0.75}{d^2}\right)y_2+\left(\frac{1.00}{9.00d}\right) \tag{8}$$

$$a_3=-\left(\frac{2.50}{d^3}\right)y_1+\left(\frac{1.00}{d^3}\right)y_2-\left(\frac{1.00}{6.00d^2}\right) \tag{9}$$

$$a_4=\left(\frac{0.50}{d^4}\right)y_1-\left(\frac{0.25}{d^4}\right)y_2+\left(\frac{1.00}{18.00d^3}\right) \tag{10}$$

Now, by varying the control points y_1 and y_2 through the GA, the values of the coefficients can be varied and consequently, various shapes of the diffuser can be obtained.

C^1 continuity both at the inlet and the outlet: In this case, only one control variable, that is, y_1 is required, which denotes height of the diffuser at the mid point of the diffuser length. Accordingly, one may get the following non-zero coefficients for Equation (6):

$$a_2=\left(\frac{18.000}{10.125d^2}\right)y_1-\left(\frac{5.625}{10.125d}\right) \tag{11}$$

$$a_3=-\left(\frac{12.000}{10.125d^3}\right)y_1+\left(\frac{5.250}{10.125d^2}\right) \tag{12}$$

$$a_4=\left(\frac{2.000}{10.125d^4}\right)y_1-\left(\frac{1.000}{10.125d^3}\right) \tag{13}$$

DOI: 10.1002/fld

Without any C^1 continuity: This requires three control points y_1, y_2, y_3. For equal spacing of the control points in the axial direction, one gets the following relationships:

$$a_0 = 0 \tag{14}$$

$$a_1 = \left(\frac{5.3333}{d}\right) y_1 - \left(\frac{4.0000}{d}\right) y_2 + \left(\frac{1.7778}{d}\right) y_3 - (3.3333) \tag{15}$$

$$a_2 = -\left(\frac{7.7037}{d^2}\right) y_1 + \left(\frac{8.4444}{d^2}\right) y_2 - \left(\frac{4.1481}{d^2}\right) y_3 + \left(\frac{8.1481}{d}\right) \tag{16}$$

$$a_3 = \left(\frac{3.5555}{d^3}\right) y_1 - \left(\frac{4.7407}{d^3}\right) y_2 + \left(\frac{2.7654}{d^3}\right) y_3 - \left(\frac{5.9259}{d^2}\right) \tag{17}$$

$$a_4 = -\left(\frac{0.5267}{d^4}\right) y_1 + \left(\frac{0.7901}{d^4}\right) y_2 - \left(\frac{0.5267}{d^4}\right) y_3 + \left(\frac{1.3169}{d^3}\right) \tag{18}$$

4.3. Implementation of the computational algorithm

The algorithm has been designed, such that the GA program and the CFD software combine with each other seamlessly and data transfer takes places without any manual intervention. In this task, the main challenge lies in embedding highly structured commercial softwares like Fluent and Gambit inside an indigenously developed control loop. This has been achieved through an algorithm coded with the C programming language. The algorithm is schematically shown in Figure 3. The GA operation and the data transfer done by the algorithm are shown by the single-walled boxes, whereas the operations of Gambit and Fluent are shown by the double-walled boxes. The interfacings of the main C code with Gambit or Fluent are shown by the thick-walled boxes. Using specially designed system commands, the interfacings among GA, Gambit and Fluent are done in such a manner that no human interventation is required.

At the time of launching, Gambit and Fluent start with their respective journal files. Gambit journal file contains all the required instructions to create mesh file in their proper sequence and similarly, the Fluent journal file contains the instructions needed to solve the velocity and the pressure fields.

5. RESULTS AND DISCUSSION

The following GA parameters (obtained through a careful study) *were* found to yield the best results: uniform crossover with a probability of 0.5, bit-wise mutation with a probability of 0.01, population size of 40. Figure 4 displays the variations of the best GA fitness with the pre-defined maximum numbers of generations of the GA run. It is important to note that there is no change in the value of the best GA fitness, whenever it is run beyond 16 generations. This study confirms the convergence of the GA search.

For the implementation of Fluent, a body-fitted triangular grid arrangement has been taken as shown typically in Figure 5. Before running the optimization algorithm, simulation of fluid in a diffuser geometry with a sudden expansion at its midway has been tried. The streamline pattern obtained by this exercise is shown in Figure 6. C_p^* value has been obtained as 0.34 for this shape.

DOI: 10.1002/fld

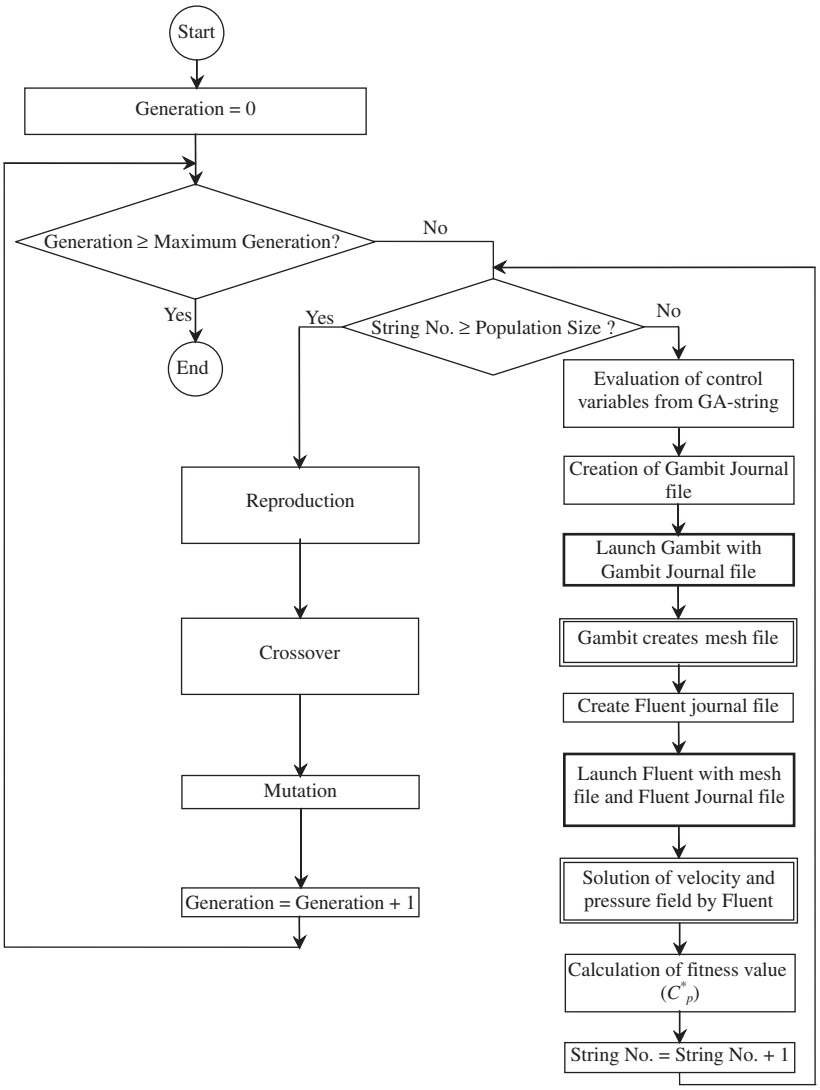

Figure 3. A schematic showing the proposed methodology to solve the problem.

One may note a prominent separation bubble at the top most corner just after the expansion. It is needless to say that such a big recirculation is mainly responsible for the large pressure drop experienced in a diffuser with a sudden expansion. A gradual increase in the cross-sectional area will reduce both the separation as well as pressure drop.

5.1. Optimum design of the duct based on discrete control points

The optimum duct design as obtained by selecting a number of control points along *abc* (Figure 1) is described briefly. As mentioned earlier, the number of control points has also been varied to

DOI: 10.1002/fld

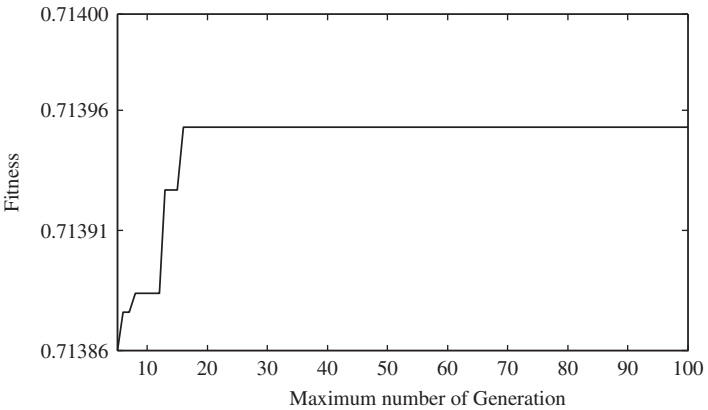

Figure 4. GA fitness versus maximum number of generation.

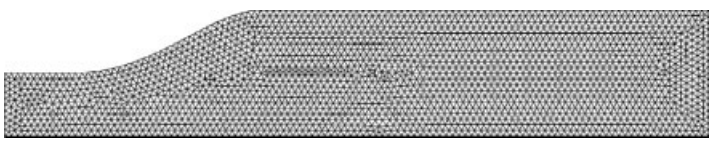

Figure 5. A typical example of the grid (one half of a planar symmetric diffuser).

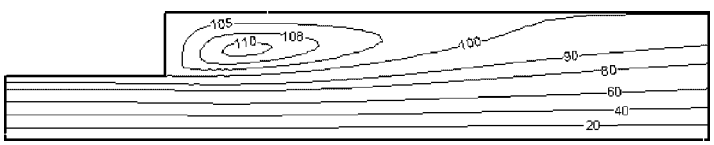

Figure 6. Streamline pattern in the diffuser with a sudden expansion.

explore various design options. The coordinate values have been obtained as the function of inlet half-width (d) to generalize the optimum solution. Table I shows the C_p^* values obtained with different number of control points and their optimal positions.

It is interesting to note that an increase in the number of control points does not increase C_p^* monotonically. The magnitude of C_p^* starts falling, if the number of control points is more than four. This is also depicted in Figure 7.

At this point, the performance of the optimum diffuser may be compared with that of a stepped diffuser (Figure 6) to assess the benefit of the optimum design. It may be recalled that a value of C_p^* for a stepped diffuser has been obtained as 0.34. Compared with that, any design shown in Table I shows a phenomenal improvement. Figure 8 shows the variation of the centreline velocity for a stepped diffuser vis-à-vis the optimum diffuser. In case of optimum diffuser, the velocity profile develops rapidly and the centreline velocity becomes constant within a small distance from the diffuser end. Finally, Figure 9 depicts the velocity profile at the diffuser end for the above two cases. The velocity profile in the stepped diffuser is highly non-uniform with a large recirculation zone at the top wall. This also corroborates the streamline pattern shown in Figure 6.

DOI: 10.1002/fld

Table I. Values of C_p^* with different number of control points and their optimal positions.

Case	Curve wall length	C_p^* value	Points no.	x coordinate	y coordinate
Single control point	3.44d	0.716660	1st	1.245d	1.026d
Two control points	3.45d	0.716725	1st	1.534d	1.059d
			2nd	3.613d	1.761d
Three control points	3.45d	0.716562	1st	1.690d	1.094d
			2nd	2.986d	1.504d
			3rd	3.872d	1.915d
Four control points	3.43d	0.717127	1st	1.415d	1.046d
			2nd	2.343d	1.265d
			3rd	3.214d	1.556d
			4th	3.909d	1.919d
Five control points	3.43d	0.714348	1st	1.570d	1.112d
			2nd	2.197d	1.353d
			3rd	2.794d	1.595d
			4th	3.394d	1.807d
			5th	3.905d	1.955d
Six control points	3.42d	0.713986	1st	1.258d	1.043d
			2nd	1.969d	1.269d
			3rd	2.488d	1.501d
			4th	2.969d	1.667d
			5th	3.426d	1.801d
			6th	3.831d	1.953d

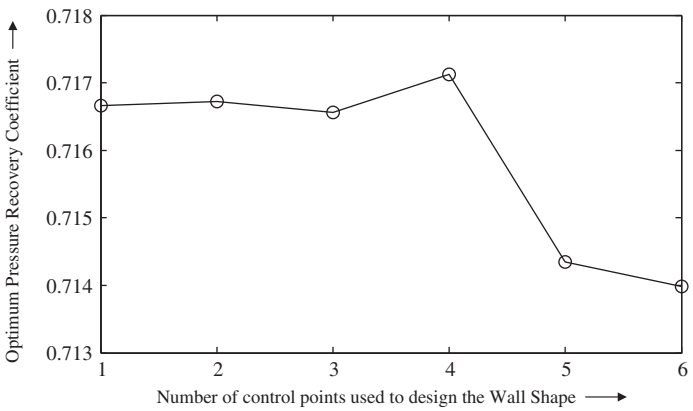

Figure 7. Variation of C_p^* with the number of control points used.

To have a better appraisal for the various optimum designs presented in Table I, streamline pattern for the six different cases is shown in Figure 10. In all the six cases, one can observe a smooth fanning of streamlines from a half-width d to the half-width $2d$ without any separation. A sharp contrast between the streamline patterns for the duct with a sudden expansion (Figure 6) and for those with optimum profile can be appreciated. It is more interesting to note the gradual

DOI: 10.1002/fld

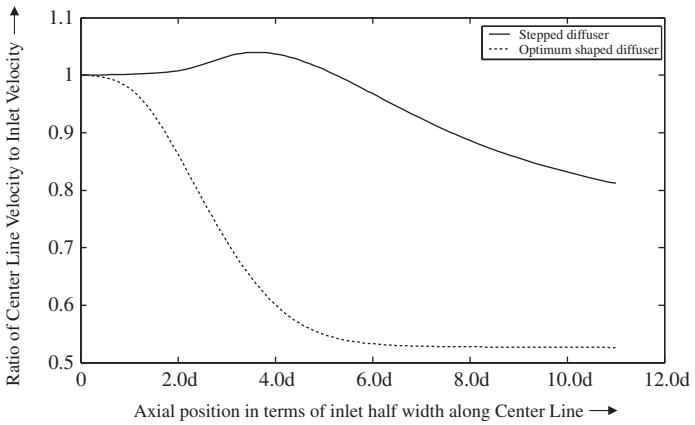

Figure 8. Variation of centerline velocity in the axial direction from the inlet of duct.

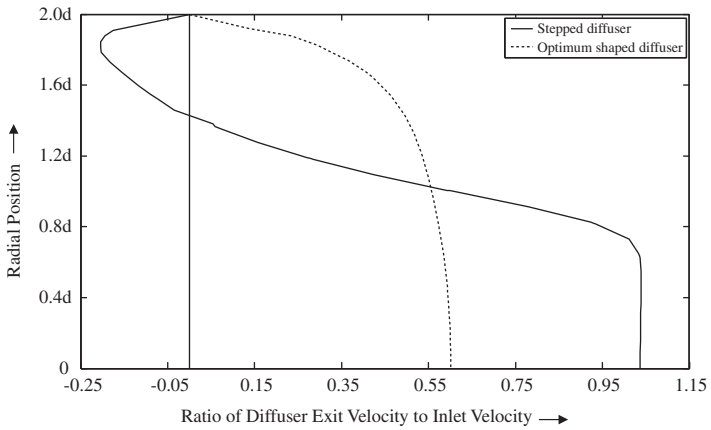

Figure 9. Velocity profiles at the diffuser exit.

change of duct profile with the increase of control points. The angles both at '*a*' and '*c*' (refer to Figure 1) become steeper, as the number of control points is increased. Further, the curve *abc* transforms from a concave one to a convex one, as the number of control points goes above four. For five and six numbers of control points, the diffuser cone takes a bell shape. With this shape, there is a gradual decrease in C_p^* according to the present simulation.

Madsen *et al.* [25] performed the shape optimization of a diffuser through the response surface technique. They obtained bell-shaped duct as the optimum design. The optimum C_p^* value obtained by them is marginally different from that obtained in the present exercise. However, there is some difference in the fluid flow simulation in these two cases. Further, the boundary conditions are also not identical. For example, they have considered a fully developed flow at the outlet, whereas the present simulation considers a pressure boundary condition. The obtained results also do not indicate a fully developed flow. This may be the probable cause of slight mismatch between the two

DOI: 10.1002/fld

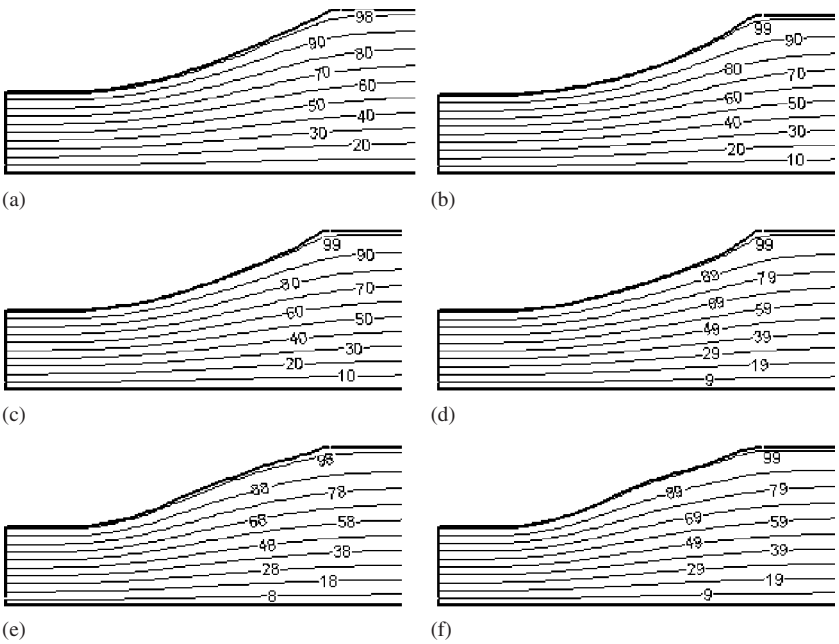

Figure 10. Optimum half shape of the diffuser and the corresponding streamline pattern for different control points: (a) single control point; (b) two control points; (c) three control points; (d) four control points; (e) five control points; and (f) six control points.

simulations. An attempt has also been made to check the correctness of the present simulation. The optimum shape obtained by Madsen *et al.* [25] has been used in our CFD model. The estimated C_p^* , thus obtained, is found to be lower than that predicted by Madsen *et al.* [25] as well as that calculated corresponding to the optimum shape obtained in the present problem.

Table I also presents the length of the diffuser wall for the different cases. Except for the case of single control point, there is a gradual decrease in the wall length, as the number of control points increases. However, the changes in both the value of C_p^* and wall length for different cases of optimum design are marginal. This gives a confidence in achieving the optimum design through GA.

In the above exercise, diffuser length has been kept fixed to $3d$ and the optimum shape has been obtained. It is obvious that the maximum value of C_p^* depends on this length and a length of $3d$ need not be the best choice. Next, an investigation has been made by varying the diffuser length. Four additional lengths $2d$, $4d$, $5d$ and $7d$ have been considered and the optimum shapes have been obtained following the methodology already outlined in the above section. Interestingly, in all the four cases, the maximum value of C_p^* has been obtained for four control points. The results of this investigation have been shown in Figure 11.

It is observed that the C_p^* value increases with the diffuser length. The trend is not surprising, as with a larger length of the diffuser the streamlines smoothly fan out from a lower to a higher cross-section, as can be seen from the streamline plot given in Figure 12. This reduces the possibility of flow separation. However, it can also be seen that the rate of increment in C_p^* diminishes with the gradual increase in diffuser length. The criteria become the maximum at a diffuser length of

DOI: 10.1002/fld

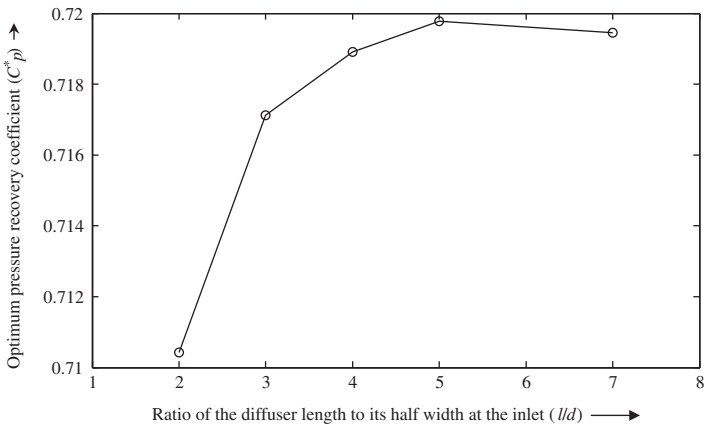

Figure 11. Variations of the highest value of optimum pressure recovery coefficient (C_p^*).

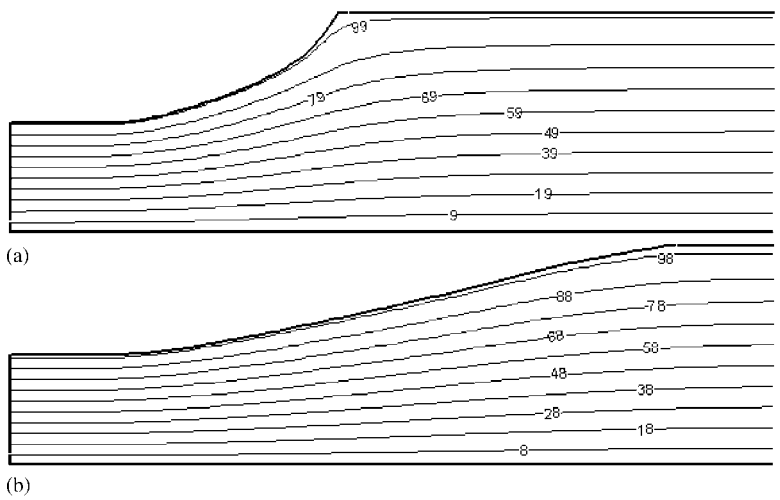

Figure 12. Optimum half shape of the diffuser and the corresponding streamline pattern: (a) diffuser length as $2d$ and (b) diffuser length as $5d$.

$5d$ but show a drooping trend, when the length is increased further to $7d$. An increase in length of the diffuser beyond a certain limit may give a marginal advantage in the reduction of form drag but increases skin friction. In most of the practical applications, the maximum allowable length of the diffuser is limited. As the optimization algorithm is generic in nature, one can try any length of the diffuser, but the final selection should depend on constraints such as available space, system layout, etc.

DOI: 10.1002/fld

Table II. The optimum position of the control points or design variables.

Case	C_p^* value	Variable	Value of the variable
C^1 continuity at the inlet only	0.716338	y_1	0.20001d
		y_2	0.51406d
C^1 continuity both at inlet and outlet	0.713953	y_1	0.38686d
Without any C^1 continuity	0.716936	y_1	0.13439d
		y_2	0.35239d
		y_3	0.61944d

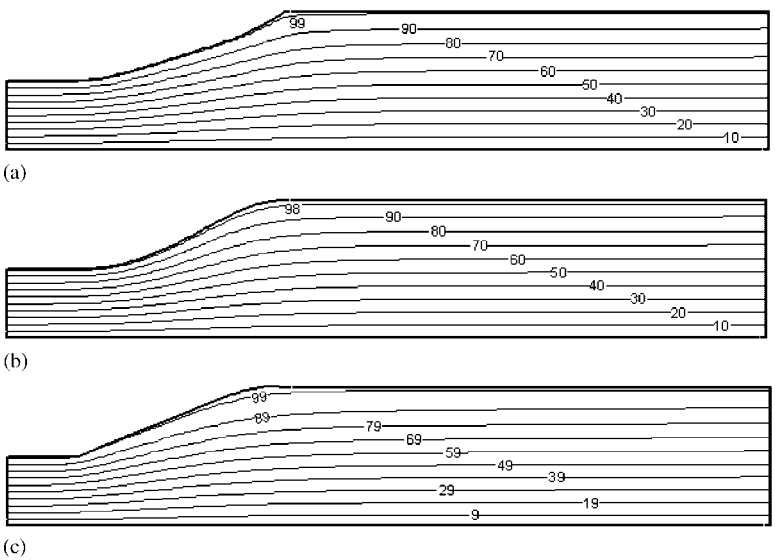

Figure 13. Optimum shape of the diffuser based on a polynomial curve and corresponding streamline patterns: (a) C^1 continuity only at inlet; (b) C^1 continuity at inlet and outlet; and (c) without any C^1 continuity.

5.2. Optimum design of the duct based on polynomial curves

Optimum positions of the control points or design variables for three different cases (C^1 continuity at inlet only, C^1 continuity both at inlet and outlet and without applying any C^1 continuity) with their corresponding pressure recovery coefficients (C_p^*) are shown in Table II. The corresponding streamline patterns are displayed in Figure 13.

It may be noted that though the changes in C_p^* value in the three cases are marginal, the highest value is obtained when C^1 continuity is relaxed both at inlet and outlet. Although the use of C^1 continuity implies a smooth transition both at the inlet and outlet, it also reduces the number of parameters to be optimized through a GA. In other words, the flexibility of the curve, which describes the wall of the diffuser, is scarified to a great extent. This results in a loss in the performance of the diffuser.

DOI: 10.1002/fld

Figure 14. Streamline pattern in the linear diffuser.

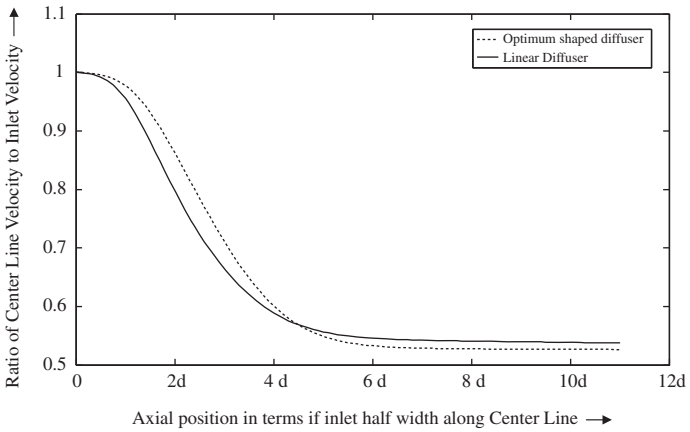

Figure 15. Variation of centerline velocity in axial direction from the inlet of duct.

5.3. Performance of a linear diffuser

The above exercise shows that the optimum diffuser essentially has curved walls. Therefore, the gain in pressure recovery is achieved through a penalty in manufacturing difficulty and cost. It would be prudent to check the performance of a diffuser with straight walls, vis-à-vis that of the optimum diffuser with curved wall. The geometry of such a diffuser is obtained by joining inlet and outlet sections with straight walls. We call this diffuser as a linear diffuser. The performances of the linear diffuser are provided in Figures 14–16. The streamline pattern shown in Figure 14 depicts a gradual deceleration of the flow and absence of any flow separation. Figure 15 shows the change in centreline velocity in the linear diffuser, while Figure 16 presents the velocity profile at the diffuser outlet. These two figures also contain the similar information of the optimum diffuser for the sake of comparison. It may be observed that both the diffusers have almost identical centreline velocity and outlet velocity profile.

This exercise shows that a linear diffuser is only marginally inferior to an optimal diffuser, whereas it presents a much simpler design. It is interesting to note that similar simplification of design is also possible in other examples of shape optimization. A parabolic shape of straight fin gives the maximum heat duty, whereas a straight-tapered fin with the same base and length transfers almost equal amount of heat in spite of its much simpler design.

DOI: 10.1002/fld

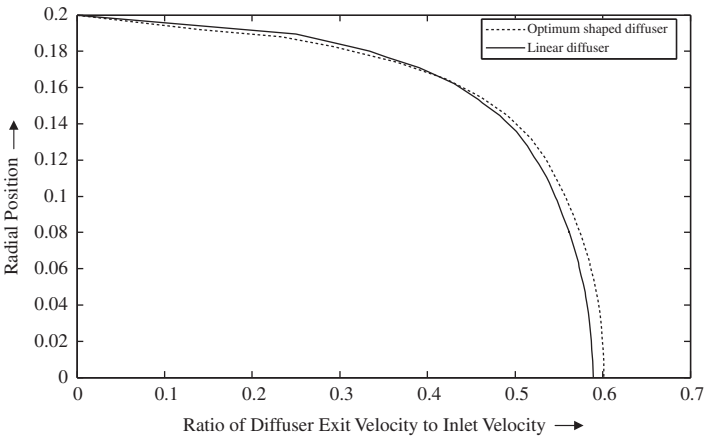

Figure 16. Velocity profile at the diffuser exit.

6. CONCLUSIONS

A comprehensive exercise has been made to find the shape of symmetric planar diffusers for attaining the maximum C_p^*. A GA has been used as the methodology of optimization. Computation of C_p^* has been made using the Gambit and Fluent softwares. An indigenous algorithm has been developed for this study, which performs a numbers of functions. It not only executes the GA but also drives the Fluent and Gambit. By some specially designed system commands, it creates the interface among GA, Gambit and Fluent in a manner, such that no human interventation is required. Special care has been taken to try different options for the diffuser geometry, so that the optimum design is not biased by the selection of initial shapes.

For achieving a globally optimum design, two different approaches have been taken. In the first approach, the control points have been directly used after deriving from the GA-string to construct the curve representing the wall shape. In this approach, the number of control points has been varied to cover a large enough search space. In the second approach, the contour of the curved section of the diffuser wall has been described by a fourth-order polynomial. In this exercise, the coefficients of the polynomial equation have been evaluated using the control points obtained from the GA-string. Optimum shapes have been obtained by constructing the curved diffuser wall in three different ways.

The salient outcomes of the present exercise are illustrated below.

- The optimum diffuser shows a substantial improvement compared with the stepped diffuser. This can be substantiated through a comparison of C_p^* values and the velocity fields in the down of the diffuser.
- Though various approaches have been taken for the optimization of duct shape, variations in C_p^* values for different optimum shapes are not found to be substantial. This not only signifies a high level of confidence for the selected design but also demonstrates the strength of GA.
- In the first approach, it has been observed that too many control variables increase the computational time required but do not guarantee a better design. Again by using too few a variables, a limited range of shape alternatives is examined. Therefore, a wide range of shape

DOI: 10.1002/fld

defined by a relatively small number of parameters is the most suitable strategy for achieving the optimum design. Here, four number of control points is found to be the best option.

- C_p^* value increases with the diffuser length, but the rate of increment in C_p^* diminishes with the gradual increase in diffuser length. It becomes the maximum at a diffuser length of $5d$ but shows a drooping trend, when the length is further increased to $7d$.
- In the second approach, the maximum C_p^* is obtained when the polynomial equation is used without any C^1 continuity. Imposition of C^1 continuity acts as an additional constraint to the selected shapes of the curves. This adversely affects the optimum design.
- Finally, the performance of a linear diffuser has also been simulated using Fluent. The performance of the linear diffuser is found to be marginally inferior only to that of an optimal diffuser. It is, therefore, left to the discretion of the designer whether to select geometry that is easier to manufacture at the cost of an incremental pressure gain.

The developed methodology is a generic one and is not restricted to the optimization of only a diffuser. The shape optimization of diverse thermo-fluids devices can be done readily with a suitable modification of the CFD simulation. For example, problems involving augmentation of heat transfer, design of chemical reactors and aerofoil shape in a cascade can be solved using the similar methodology. The techniques used for combining Fluent with the indigenously developed optimization algorithm can also be utilized in principle with others applications like combining two altogether different commercial softwares.

REFERENCES

1. Padra C. The beginnings of variational calculus, and its early relation with numerical methods. In *Variational Formulations in Mechanics*: *Theory and Applications*, Toroco E, de Souza Neto, Novotny AA (eds). c CIMINE, Barcelona, Spain, 2006.
2. Desaix M, Anderson D, Lisak M. The brachistochrone problem—an introduction to variational calculus for undergraduate students. *European Journal of Physics* 2005; **26**:857–864.
3. Fabbri G. Heat transfer optimization in corrugated wall channels. *International Journal for Heat and Mass Transfer* 2006; **43**(23):4299–4310.
4. Fabbri G. Heat transfer optimization in internally finned tubes under laminar flow conditions. *International Journal for Heat and Mass Transfer* 1998; **41**(8):1243–1253.
5. Fabbri G. Effect of viscous dissipation on the optimization of the heat transfer in internally finned tubes. *International Journal for Heat and Mass Transfer* 2004; **47**(14–16):3003–3015.
6. Lee KS, Kim WS, Si JM. Optimal shape and arrangement of staggered pins in the channel of a plate heat exchanger. *International Journal for Heat and Mass Transfer* 2001; **44**(17):3223–3231.
7. Matos RS, Vargas JVC, Laursen TA, Bejan A. Optimally staggered finned circular and elliptic tubes in forced convection. *International Journal for Heat and Mass Transfer* 2004; **47**(6–7):1347–1359.
8. Okabe T, Foli K, Olhofer M, Jin Y, Sendhoff B. Comparative studies on micro heat exchanger optimization. *Proceedings of the IEEE Congress on Evolutionary Computation*, Canberra, Australia, vol. 1, 2003; 647–654.
9. Mohammadi B, Pironneau O. *Applied Shape Optimization for Fluids*. Oxford University Press: Oxford, 2001.
10. Dulikravich GS. Aerodynamic shape design and optimization. *AIAA Paper No. 91-0476*, 1991.
11. Falco ID. *An Introduction to Evolutionary Algorithms and their Application to the Aerofoil Design Problem—Part I*: *The Algorithms*. Von Kármán Lecture Series on Fluid Dynamics. von Kareman Institute: Rhode-Saint-Genese, Bruxelles, Belgium, 1997.
12. Mäkinen R, Neittaanmäki P, Périaux J, Toivanen J. A genetic algorithm for multiobjective design optimization in aerodynamics and electromagnetics. In *Computational Fluid Dynamics '98*, *Proceedings of the ECCOMAS 98 Conference*, Papailiou KD, Tsahalis D, Périaux J, Knörzer D (eds), vol. 2. Wiley: Athens, Greece, 1998; 418–422.
13. Baysal O, Eleshaky M. Aerodynamic design optimization using sensitivity analysis and computational fluid dynamics. *AIAA Journal* 1992; **30**:718–725.

DOI: 10.1002/fld

14. Reuther J, Jameson A, Alonso J, Rimlinger M, Saunders D. Constrained multipoint aerodynamic shape optimization using an adjoint formulation and parallel computers. *Part 1*, *Journal of Aircraft* 1999; **36**:51–60.
15. Reuther J, Jameson A, Alonso J, Rimlinger M, Saunders D. Constrained multipoint aerodynamic shape optimization using an adjoint formulation and parallel computers. *Part 2*, *Journal of Aircraft* 1999; **36**:61–74.
16. Bängtsson E, Noreland, D, Berggren M. Shape optimization of an acoustic horn. *Computer Methods in Applied Mechanics and Engineering* 2003; **192**:1533–1571.
17. Mohammadi B, Molho J, Santiago J. Incomplete sensitivities for the design of minimal dispersion fluidic channels. *Computer Methods in Applied Mechanics and Engineering* 2003; **192**:4131–4145.
18. Han SY, Maeng JS. Shape optimization of cut-off in a multi-blade fan/scroll system using neural network. *International Journal for Heat and Mass Transfer* 2003; **46**(15):2833–2839.
19. Lehnhauser T, Schafer M. A numerical approach for shape optimization of fluid flow domains. *Computer Methods in Applied Mechanics and Engineering* 2005; **194**:5221–5241.
20. Kline SJ, Abbott DE, Fox RW. Optimum design of straight-walled diffusers. *Journal of Basic Engineering* 1959; **81**:321–329.
21. Reneau LR, Johnston JP, Kline SJ. Performance and design of straight, two-dimensional diffusers. *Journal of Basic Engineering* 1967; **89**:141–150.
22. Carlson JJ, Johnston JP, Sagi CJ. Effects of wall shape on flow regimes and performance in straight, two-dimensional diffusers. *Journal of Basic Engineering* 1967; **89**:151–160.
23. Cabuk H, Modi V. Optimum plane diffusers in laminar flow. *Journal of Fluid Mechanics* 1992; **237**:373–393.
24. Svenningsen KH, Madsen JI, Päuker WHG, Hassing NH. Optimization of flow geometries applying quasi-analytical sensitivity analysis. *Applied Mathematical Modelling* 1996; **20**(N3):214–224.
25. Madsen JI, Shyy WR, Haftka T. Response surface techniques for diffuser shape optimization. *AIAA Journal* 2000; **38**(7):1512–1518.
26. Maeng JS, Han SY. Application of the growth-strain method for shape optimization of flow systems. *Numerical Heat Transfer*, *Part A* 2004; **45**:235–246.
27. Fan HY, Dulikravich GS, Han ZX. Aerodynamics data modeling using support machines. *Inverse Problem in Science and Engineering* 2005; **13**(N3):261–278.
28. Goel T, Dorney DJ, Haftka RT, Shyy W. Improving the hydrodynamic performance of diffuser vanes via shape optimization. *The 43rd AIAA/ASME/SAE/ASEE Joint Propulsion Conference and Exhibit*, Cincinnati, OH, 2007.
29. Fluent Inc., *FLUENT 6.3 User's Guide*. Fluent Inc., 2006.
30. Fluent Inc., *GAMBIT 2.3 User's Guide*. Fluent Inc., 2006.
31. Pratihar DK. *Soft Computing*. Narosa Publishing House: New Delhi, India, 2008.
32. Holland JH. *Adaptation in Natural and Artificial Systems*. The University of Michigan Press: Ann Arbor, MI, U.S.A., 1975.
33. Goldberg DE. *Genetic Algorithms in Search*, *Optimization and Machine Learning*. Addison-Wesley: Reading, MA, 1989.
34. Launder BE, Spalding DB. *Lectures in Mathematical Models of Turbulence*. Academic Press: London, England, 1972.
35. Launder BE, Spalding DB. The numerical computation of turbulent flows. *Computer Methods in Applied Mechanics and Engineering* 1974; **3**:269–289.

DOI: 10.1002/fld